LANDING SITE ASSESSMENT FOR AN AUSTRALIAN ROVER NEAR THE LUNAR SOUTH POLE

K. Hoza[1], [1]First Mode, kathleen@firstmode.com

Introduction: The lunar South Pole is a compelling target for exploration and science because of features including a rich volatile resource inventory, an ancient and deeply cratered surface, and unique interactions between the lunar surface and the space weathering environment. As such, the Australian Space Agency's first spaceflight mission, a 20 kg technology demonstration rover named Roo-ver, will be designed to operate within 10° of the lunar South Pole.

However, the lunar South Pole also poses challenges for rover operations, particularly with regards to illumination and thermal conditions, which are highly variable with local topography due to the Moon's minimal axial tilt of 1.54°. Despite global interest in the South Polar region, no rover has yet operated south of -70° on the lunar surface.

Here, we present a methodology and demonstrate its application for preliminary assessment of two possible landing sites near the lunar South Pole. Although benign landing sites may not be common at extreme latitudes, results suggest there are locations where a small rover could safely operate even in very close proximity to the South Pole.

Landing Site Assessment Methodology: Landing sites were evaluated on the basis of hazards posed to a small rover, with the Australian Space Agency's technology demonstration objective assumed to be equally achievable at all sites where a rover can safely operate.

Slope and roughness hazards. Features shorter than the rover baselength (~0.5 m) are considered roughness hazards and those longer than the rover baselength are considered slope hazards as per [1]. Slopes apparent in [2] were used to rule out any site with a slope of > 5° on baselengths ranging from 5-60 m. Similarly, large fresh impact craters are likely to be surrounded by boulder fields and were avoided (e.g. [3]).

Small-scale rocks and craters not detectable from orbit could pose additional roughness and slope hazards. We consider the possibility of inferring the distribution of small-scale rocks and craters from larger features and quantify the likely distribution of these hazards at sites selected to be as safe as reasonably possible.

Crater distribution. Small craters with diameter less than 200 m are expected to have reached an equilibrium state everywhere on the lunar surface. In this regime, each new impact destroys on average as many craters as it creates, and crater frequency is modelled to follow Equation 1 where $N_{Equilibrium}$ represents the number of craters per unit area with diameter equal or greater than diameter D [4].

$$N_{Equilibrium} = 0.079433D^{-2} \quad (1)$$

Assessing the navigational risk posed by a crater to a rover requires estimating its depth and approximate morphology as well as the crater diameter. Previous studies have quantified how crater depths and wall slopes degrade over time (e.g.[5]) and the dependence of fresh crater depth and wall slope on crater size (e.g. [6]).

Here, these results are synthesized to generate a representative expected distribution of crater size, depth, and wall slope, expected to be a valid approximation for any landing site on the lunar surface (**Figure 1**).

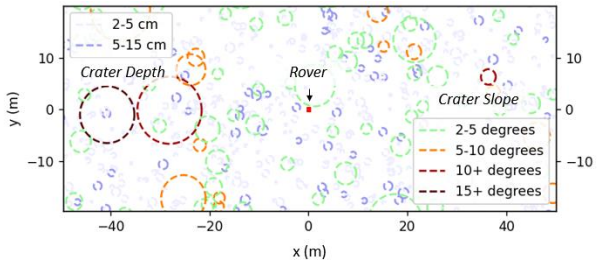

Figure 1: Representative crater distribution assuming Trask Equilibrium size-frequency distribution, fresh crater morphology as per [6], and crater degradation as per [5].

As a preliminary validation of this approach, simulated craters 6m and larger were compared against craters of the same size range, which are easily resolvable in LRO NAC imagery, at a site on the lunar surface (**Figure 2**).

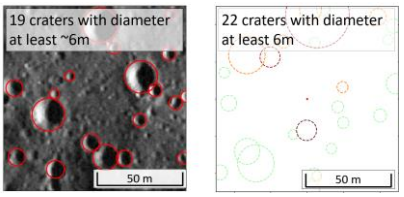

Figure 2: Craters on the lunar surface (left) as compared to simulated craters (right).

Rock abundance. Rock size-frequency distributions are commonly modeled to follow exponential relationships on bodies where wind and water dominate erosion [7] and power law relationships on bodies where impact comminution dominates [3]. However, a power law extrapolation from m-scale rocks observed in LRO NAC images of 7 sites is found to consistently overestimate the abundance of cm-scale rocks observed in situ at the same sites (**Figure 3**).

Furthermore, m-scale rockiness appears to be a poor qualitative indicator of cm-scale rockiness, with the highest m-scale rock abundance at Chang'e 3 mapping to the lowest cm-scale rock abundance.

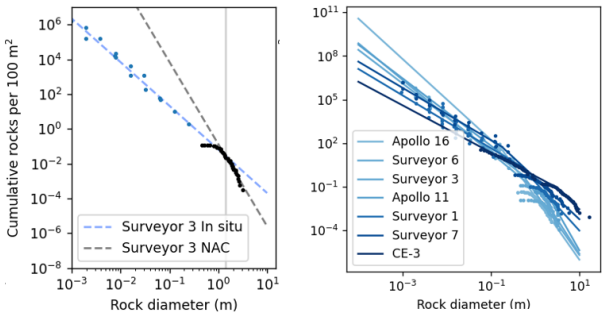

Figure 3: Left: A power law relationship cannot be used to extrapolate from m-scale rocks to cm-scale rocks at the Surveyor 3 landing site. Right: Similar analysis including 6 additional sites. NAC measurements below about 1 m are assumed to be affected by the resolution limit of the camera and ignored.

One possible explanation for these observations has been posited by [8], who suggest that although large impact craters generate rocks following power law distributions, subsequent rock destruction processes break down smaller rocks faster than large ones, resulting in rocks on old surfaces deviating from a power law distribution. More detailed future work in this area could potentially enable inference of small-scale rock distribution based on the age of lunar surface features in combination with m-scale boulder observations.

In the meantime, m-scale boulder count is not used as a criterion for landing site selection. Instead, we assume that cm-scale rockiness will remain largely unknown until the time of landing but will be the same or less than rockiness observed at the Apollo 11 site, which at the cm-scale is the rockiest site not located near a large fresh impact crater.

Thermal and illumination environment. Thermal and illumination environments near the lunar poles are highly dependent on local topography and season. To complement published maximum and minimum temperature maps [9], we additionally use LROC WAC images [10] and LRO Diviner TIR data [11] to plot surface temperature and illumination as a function of time of lunar day and season at each evaluated landing site. Some illumination is required for a site to be a viable candidate, and sites with extended periods of illumination are preferred. Other than extremely cold PSRs, thermal observations are not used as a constraint, but rather to inform what maximum and minimum temperatures should be used as the basis for rover thermal design at any given landing site. In future work, these historical datasets could be further supplemented by mapping the horizon line at a location of interest and evaluating local solar visibility for the specific dates relevant to a given mission profile.

Landing Site A is located at (85.06° S, 9.76° E) in Malapert crater. Slope on a 5-m baselength is 1° [2]. Earth visibility is 50% [12]. Thermal and illumination characteristics, shown below, are acceptable during summer months. In the winter, the illuminated period might be as short as 1 lunar hour (1/24 of 1 lunar day), ruling this out as a viable winter landing site.

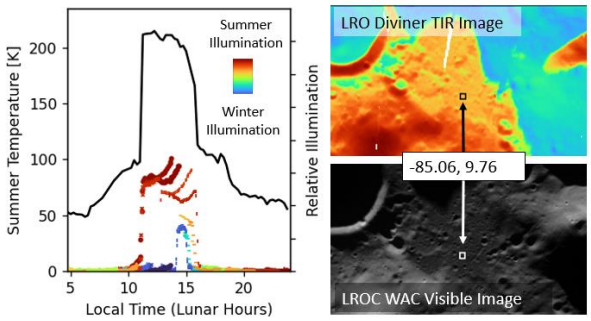

Landing Site B is located at 89.44° S, 137.29° W on the Shackleton connecting ridge. Slope on a 5-m baselength is 4° [2]. Earth visibility is 58% [12]. Thermal and illumination characteristics are acceptable throughout the year.

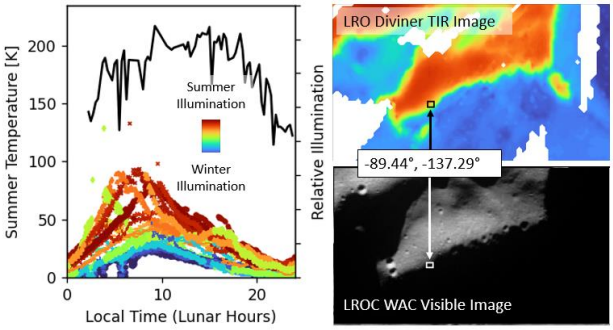

References: [1] De Rosa D. et al (2012) *Planetary and Space Science* 74, 224-246. [2] Barker, M.K., et al. (2021), Planetary & Space Science 203, 105119 (LROC QuickMap). [3] Bandfield J. L. et al (2011) *JGR*, 116, E12. [4] NASA SLS Spec-159 Rev G. [5] Basilevsky A. T. (1976) *Proc Lunar Sci. Conf. 7* p.1005-1020 [6] Cai Y. and Fa W. (2020) *JGR: Planets*, 125. [7] Golombek M.P. et al (2002) *JGR* E12, 8086 [8] Ruesch O. et al (2022) *Icarus 387* 115200 [9] Williams, J.-P. et al. (2019). *JGR: Planets 124*, 2505–2521. [10] LRO-L-LROC-5-RDR-V1.0 *NASA PDS*. 10.17189/1520341 [11] Williams, J.-P. et al (2019). LRO-L-DLRE-5-GCP-V1.0. *NASA PDS* 10.17189/1520655 [12] Mazarico E. et al. (2011). *Icarus 211* 1066-1081, (LROC QuickMap).